

# **SANDIA REPORT**

SAND2001-3619

Unlimited Release

Printed November 2001

## **Embedded Self-Powered MicroSensors for Monitoring the Surety of Critical Buildings and Infrastructures**

K. B. Pfeifer, S. K. Leming, and A. N. Rumpf

Prepared by  
Sandia National Laboratories  
Albuquerque, New Mexico 87185 and Livermore, California 94550

Sandia is a multiprogram laboratory operated by Sandia Corporation,  
a Lockheed Martin Company, for the United States Department of  
Energy under Contract DE-AC04-94AL85000.

Approved for public release; further dissemination unlimited.



**Sandia National Laboratories**

Issued by Sandia National Laboratories, operated for the United States Department of Energy by Sandia Corporation.

**NOTICE:** This report was prepared as an account of work sponsored by an agency of the United States Government. Neither the United States Government, nor any agency thereof, nor any of their employees, nor any of their contractors, subcontractors, or their employees, make any warranty, express or implied, or assume any legal liability or responsibility for the accuracy, completeness, or usefulness of any information, apparatus, product, or process disclosed, or represent that its use would not infringe privately owned rights. Reference herein to any specific commercial product, process, or service by trade name, trademark, manufacturer, or otherwise, does not necessarily constitute or imply its endorsement, recommendation, or favoring by the United States Government, any agency thereof, or any of their contractors or subcontractors. The views and opinions expressed herein do not necessarily state or reflect those of the United States Government, any agency thereof, or any of their contractors.

Printed in the United States of America. This report has been reproduced directly from the best available copy.

Available to DOE and DOE contractors from  
U.S. Department of Energy  
Office of Scientific and Technical Information  
P.O. Box 62  
Oak Ridge, TN 37831

Telephone: (865)576-8401  
Facsimile: (865)576-5728  
E-Mail: [reports@adonis.osti.gov](mailto:reports@adonis.osti.gov)  
Online ordering: <http://www.doe.gov/bridge>

Available to the public from  
U.S. Department of Commerce  
National Technical Information Service  
5285 Port Royal Rd  
Springfield, VA 22161

Telephone: (800)553-6847  
Facsimile: (703)605-6900  
E-Mail: [orders@ntis.fedworld.gov](mailto:orders@ntis.fedworld.gov)  
Online order: <http://www.ntis.gov/ordering.htm>



***Embedded Self-Powered MicroSensors for Monitoring the  
Surety of Critical Buildings and Infrastructures***

***K. B. Pfeifer, S. K. Leming***

***Microsensor Science and Technology***

***Sandia National Laboratories***

***P. O. Box 5800***

***Albuquerque, NM 87185-1425***

***A. N. Rumpf***

***L&M Technologies Corporation***

***Albuquerque, NM***

**Abstract**

Monitoring the condition of critical structures is vital for not only assuring occupant safety and security during naturally occurring and malevolent events, but also to determine the fatigue rate under normal aging conditions and to allow for efficient upgrades. This project evaluated the feasibility of applying integrated, remotely monitored micro-sensor systems to assess the structural performance of critical infrastructure. These measurement systems will provide forensic data on structural integrity, health, response, and overall structural performance in load environments such as aging, earthquake, severe wind, and blast attacks.

We have investigated the development of "self-powered" sensor tags that can be used to monitor the state-of-health of a structure and can be embedded in that structure without compromising the integrity of the structure. A sensor system that is powered by converting structural stresses into electrical power via piezoelectric transducers has been demonstrated including work toward integration of that sensor with a novel radio frequency (RF) tagging technology as a means of remotely reading the data from the sensor.

## **TABLE OF CONTENTS**

<b>ABSTRACT</b>	<b>3</b>
<b>TABLE OF CONTENTS</b>	<b>4</b>
<b>TABLE OF FIGURES</b>	<b>5</b>
<b>INTRODUCTION</b>	<b>6</b>
<b>MECHANICAL CALCULATIONS</b>	<b>7</b>
<b>BEAM EXPERIMENT</b>	<b>10</b>
<b>RF TAG STUDIES</b>	<b>13</b>
<b>CONCLUSION</b>	<b>14</b>
<b>REFERENCES</b>	<b>15</b>
<b>DISTRIBUTION</b>	<b>16</b>

## TABLE OF FIGURES

FIGURE 1. DIAGRAM OF SELF-POWERED SENSOR SYSTEM. THE DIAGRAM ILLUSTRATES THE PIEZOELECTRIC GENERATOR, POWER STORAGE, MICROPROCESSOR CONTROLLER, SENSOR, AND RF TAG FOR DATA STORAGE AND READOUT. ....	6
<b>FIGURE 2.</b> SCHEMATIC DIAGRAM OF POWER SUPPLY CIRCUIT. DIAGRAM ILLUSTRATES THE PIEZOELECTRIC GENERATOR, CAPACITOR ENERGY STORAGE BANKS, OVERVOLTAGE PROTECTION, AND PIC16C71 MICROPROCESSOR. ....	7
FIGURE 3. SCHEMATIC DIAGRAM OF THE LUMPED CIRCUIT MODEL OF A PIEZOELECTRIC CHARGE GENERATOR. ELEMENT CONSISTS OF AN IDEAL AC CHARGE GENERATOR, WITH A PARASITIC CAPACITANCE AND PARASITIC RESISTANCE IN PARALLEL. ....	8
FIGURE 4. DIAGRAM OF GENERATOR STRAIN EXPERIMENT ILLUSTRATING MECHANICAL MOTION OF THE GENERATOR. MAXIMUM DEFLECTION WAS CONSTRAINED TO 0.76 MM. .	8
FIGURE 5. DATA ILLUSTRATING THE RELATIONSHIP BETWEEN APPLIED FORCE AND OPEN-CIRCUIT VOLTAGE FOR THE PIEZOELECTRIC GENERATOR. ....	9
FIGURE 6. DIAGRAM OF PIEZOELECTRIC GENERATOR AND STRAIN GAUGE ON STEEL BEAM. BEAM WAS SUSPENDED FROM AN ELASTIC CABLE AND STRUCK PERPENDICULAR TO VERTICAL AXIS. ....	10
FIGURE 7. DATA PLOT SHOWING RELATIONSHIP BETWEEN OUTPUT VOLTAGE OF PIEZOELECTRIC AND STRAIN ON THE BEAM OF FIGURE 6. IT IS CLEAR THAT THE OUTPUT IS PROPORTIONAL TO THE STRAIN WITH A SLOPE OF ~14 MV/M-STRAIN. ....	11
FIGURE 8. PLOT OF RESPONSE AS A FUNCTION OF TIME FOR A RAPID IMPULSE ON A BEAM. THE DATA PLOTTED AS (●) IS THE VOLTAGE ACROSS THE CAPACITOR BANK, THE SOLID LINE DATA IS THE TRANSIENT VOLTAGE OUTPUT FROM THE PIEZOELECTRIC GENERATOR, AND THE SOLID SQUARE (■) IS THE TOTAL ENERGY ACROSS THE CAPACITOR BANK. THIS IS THE INTEGRATED ENERGY FOR ONE IMPULSE. TO FIRST ORDER, THE ENERGY SHOULD SCALE WITH THE NUMBER OF IMPULSES TO THE BEAM. NOTE THAT THE DROOP IS A RESULT OF LOADING BY THE OSCILLOSCOPE WITH A 1 MΩ INPUT IMPEDANCE AND LEAKAGE OF THE DIODES IN THE BRIDGE RECTIFIER CIRCUIT. ....	12
<b>FIGURE 9.</b> BLOCK DIAGRAM OF THE SELF-POWERED SENSOR SYSTEM ILLUSTRATING CONTACT PROGRAMMING TECHNIQUE AND CONTROL FROM THE MICROPROCESSOR. ....	12
FIGURE 10. SCHEMATIC DIAGRAM OF MCRF355 WIRED WITH AN RF RESONANT CIRCUIT. TOP DIAGRAM IS FOR A SWITCHED CAPACITANCE AND THE BOTTOM DIAGRAM IS FOR A SWITCHED INDUCTANCE SYSTEM. ....	13
<b>FIGURE 11.</b> DATA SHOWING THE IMPEDANCE FOR CIRCUITS IN FIGURE 10 AS A FUNCTION OF FREQUENCY. THE QUIESCENT FREQUENCY IS 13.56 MHZ. DATA PLOTTED AS A FILLED CIRCLE IS THE SWITCHED CAPACITOR CIRCUIT RESONANCE WITH PIN B OF THE MCRF355 INACTIVE. THE DATA PLOTTED AS THE TRIANGLE IS THE RESONANCE OF THE SWITCHED CAPACITOR CIRCUIT WHEN PIN B IS ACTIVE. THE FILLED SQUARE AND THE OPEN DIAMOND DATA ARE FOR THE SWITCHED INDUCTOR DATA WITH PIN B INACTIVE AND ACTIVE RESPECTIVELY. ....	14

**Embedded Self-Powered MicroSensors for Monitoring the  
Surety of Critical Buildings and Infrastructures**

**K. B. Pfeifer, S. K. Leming**

**Microsensor Science and Technology**

**Sandia National Laboratories**

**P. O. Box 5800**

**Albuquerque, NM 87185-1425**

**A. N. Rumpf**

**L&M Technologies Corporation**

**Albuquerque, NM**

**INTRODUCTION**

The health of critical infrastructure, as has been so recently and tragically demonstrated by the events at the

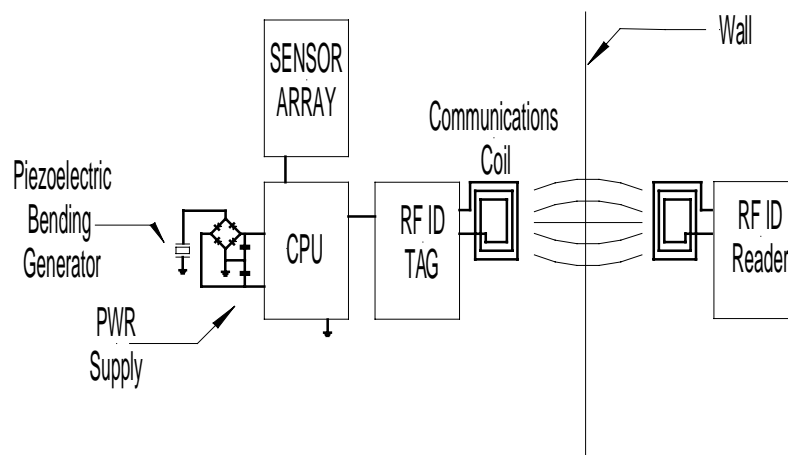


**Figure 1.** Diagram of self-powered sensor system. The diagram illustrates the piezoelectric generator, power storage, microprocessor controller, sensor, and RF tag for data storage and readout.

World Trade Center in New York City, demonstrate the need for systems that can autonomously measure the health of that infrastructure. We have investigated the application of “self-powered” sensors to the problem of long-term detection of infrastructure health by studying the feasibility of using naturally occurring load-induced strains to excite a piezoelectric generator and power a microprocessor controlled sensor system. That microprocessor would command and control a system that would make a measurement and then save the data from that measurement to a non-volatile memory. Since the strains induced by the event would be transient, enough energy would be needed to activate the microprocessor, make the measurement, and store the data before the strain event concluded. The data could then be read from the commercial off the shelf RF tag via a reader. The clear objective of this project is to develop the ability to field a sensor that has neither wires protruding from a building member nor batteries and can be embedded into a building member at fabrication. We have studied a system similar to the block diagram

shown in Figure 1, which shows a system consisting of a power supply, microprocessor, sensor, and RF tag for reading out the data.

## Mechanical Calculations

Development of a *self-powered* sensor system requires the construction of a high efficiency power supply circuit to store the charge produced by the piezoelectric element and drive the sensor system. Initially we have used a Piezo Systems, Inc.<sup>1</sup> 2.5"x1.25"x0.020" (63 mm x 31.8 mm x 0.51 mm) parallel poled piezoelectric generator connected to a full wave bridge rectifier circuit. *Figure 2-* is a schematic diagram of the basic system to test the feasibility of operating a micro-controller from a piezoelectric element. As illustrated, the charge generated during actuation of the piezoelectric element is passed into a full-wave

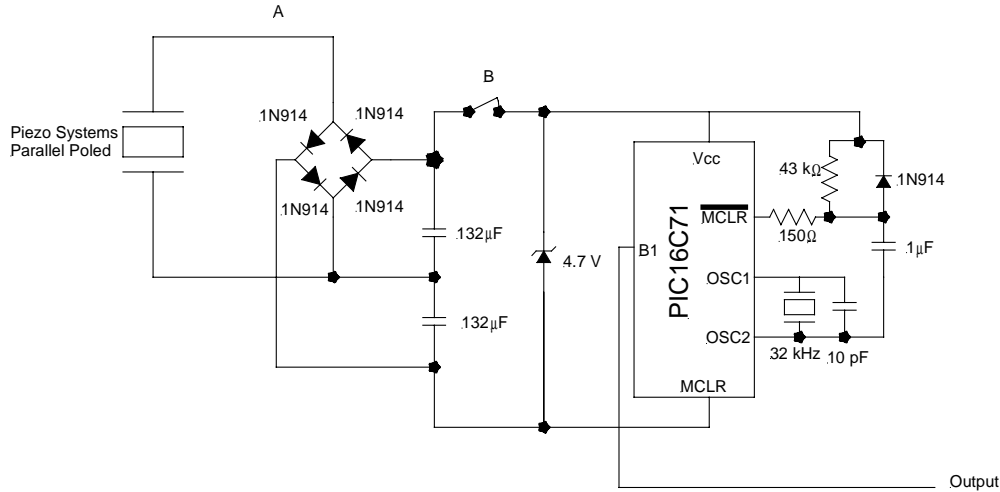


**Figure 2.** Schematic diagram of power supply circuit. Diagram illustrates the piezoelectric generator, capacitor energy storage banks, overvoltage protection, and PIC16C71 microprocessor.

bridge rectifier circuit constructed from 1N914 diodes. The 1N914 diode has a very low reverse leakage current on the order of 25 nA. Charge is then stored in the capacitance bank that is wired in a voltage doubling configuration. That voltage is limited by the 4.7 V zener diode placed across the power input to the PIC16C71 microcontroller. The PIC16C71 is programmed in the low-power (LP) mode with a 32 kHz crystal to set the processing frequency. The PIC16C71 is rated to operate at 2.5 V with approximately 15  $\mu$ A (<40  $\mu$ W) of current in its low power mode and will draw 1  $\mu$ A in programmed shutdown or “sleep” mode.

A simple circuit model of the piezoelectric generator is illustrated in Figure 3 and demonstrates the reverse leakage through the piezoelectric element. The leakage resistance of the diodes and the leakage resistance of the piezoelectric generator constitute the bulk of the losses in the power supply section of the circuit and ultimately determine the minimum frequency of the strain events required to maintain the voltage across the circuit at usable levels.

A simple experiment was conducted to determine the minimum strain required at 1 Hz to operate the microprocessor. The piezoelectric generator was positioned over two rolling rods as shown in Figure 4 and actuated manually over a maximum deflection of 0.76 mm at a constant rate of 1 Hz. It was found that the PIC16C71 oscillator became active and the firmware began sequencing after an average of 17.3 cycles (~17 sec). The average voltage required to activate the PIC16C71 was 1.518 V implying that the average total charge on the capacitance bank is on the order of:

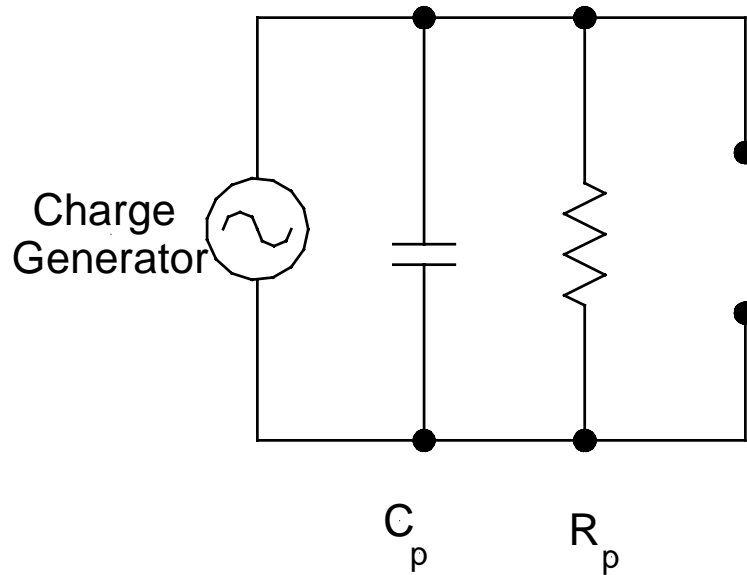


**Figure 3.** Schematic diagram of the lumped circuit model of a piezoelectric charge generator. Element consists of an ideal AC charge generator, with a parasitic capacitance and parasitic resistance in parallel.

$$Q_{tot} = CV = 264\mu F \times 1.518V = 0.4mC \quad (1)$$

$$Q_{pulse} = \frac{Q_{tot}}{N_{pulses}} = \frac{0.4mC}{17.3pulses} = 2.3 \times 10^{-5} C/pulse \quad (2)$$

Where  $Q_{tot}$  is the total stored charge,  $C$  is the total capacitance of the circuit,  $V$  is the average voltage measured at the instant the microprocessor began operation, and  $N$  is the average number of pulses required to charge the circuit to operational levels. Thus, the average charge stored per pulse is on the order of  $20 \mu C$ . It has been shown that the maximum short circuit current ( $Q_{sc}$ ) that can be delivered by the

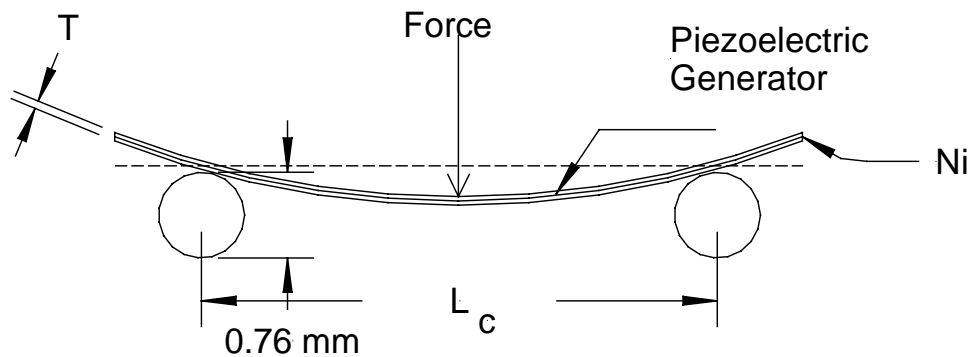


**Figure 4.** Diagram of generator strain experiment illustrating mechanical motion of the generator. Maximum deflection was constrained to 0.76 mm.

piezoelectric element is:<sup>2</sup>

$$Q_{sc} = \frac{3}{2} \left( 1 - \frac{\delta}{T} \right) \frac{bT}{L_c} Y d_{31} \Delta x \quad (3)$$

where  $\delta$  is the thickness of the Ni plate in the piezoelectric bending generator (0.3 mm),  $b$  is the width of the bending generator (0.0318 m),  $Y$  is the average Young's modulus ( $5.5 \times 10^{10} \text{ N/m}^2$ ),  $d_{31}$  is the piezoelectric transverse charge coefficient ( $-190 \times 10^{-12} \text{ m/V}$ ),  $L_c$  is the spacing between the rolling rods (0.063 m), and  $T$  is the thickness of the bending generator (0.51 mm).

Calculation of the maximum short circuit charge yields a value of  $6.1 \times 10^{-6} \text{ C}$  generated when the force is applied and  $6.1 \times 10^{-6} \text{ C}$  generated when the force is removed. Thus, the total charge stored by the

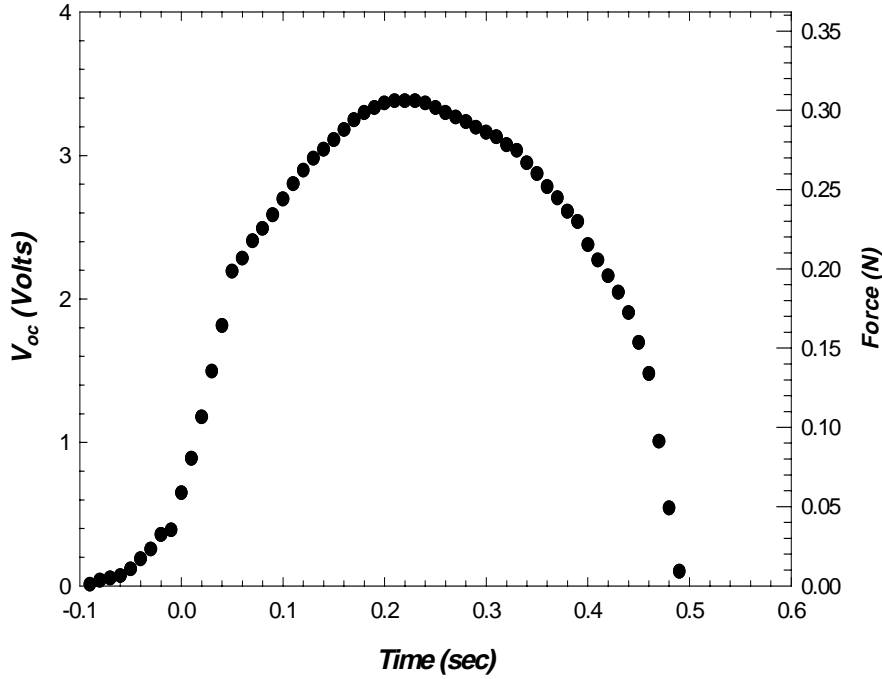


**Figure 5.** Data illustrating the relationship between applied force and open-circuit voltage for the piezoelectric generator.

capacitors is on the order of  $\sim 1.2 \times 10^{-5} \text{ C/pulse}$ . This is consistent with the value of  $20 \mu\text{C}$  calculated from the voltage above. Thus, this measurement indicates that the model and the measured behavior are consistent to within a factor of two. This implies that a reasonable calculation of the required strain necessary to power the device can be determined using the measured voltages and the models.

Recognizing that the open circuit voltage can be written in terms of force as:

$$V_{oc}(F) = \frac{3}{8} \left( 1 - \left( \frac{\delta}{T} \right)^2 \right) \frac{L_c}{bT} g_{31} F \quad (4)$$

where  $g_{31}$  is the piezoelectric transverse voltage coefficient ( $11.6 \times 10^{-3} \text{ Vm/N}$ ) and  $F$  is the applied force in Newtons allows calculation of the net force applied as a function of voltage and the required strain to operate the system. Figure 5 is a plot of the voltage (left axis) and the applied force as calculated from Eqn. (4) (right axis). This data indicates that the force applied to generate an open circuit voltage of 3.5 V is on

the order of 0.3 N. Thus, the maximum surface strain that is applied to the bending generator is on the order of  $390 \times 10^{-6}$  as calculated from Eqn. 5.

$$S_{\max} \sim \left( \frac{0.48T}{L_c^2} \right) \Delta x \quad (5)$$

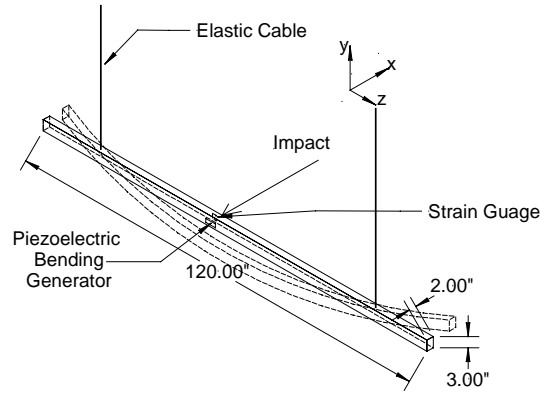


**Figure 6.** Diagram of piezoelectric generator and strain gauge on steel beam. Beam was suspended from an elastic cable and struck perpendicular to vertical axis.

Thus, an oscillating strain of  $400 \mu$ -Strain applied to the bending generator for a period of 20 sec will generate enough charge to power the microprocessor and do usable work.

### Beam Experiment

The response of the generator was then compared to a calibrated strain gauge by placing the bending generator on a  $10' \times 3'' \times 2''$  steel beam as shown in Figure 6. By exciting the beam with an impact along the  $x$ -axis as shown in the diagram and then comparing the output of the strain gauge to the output of the piezoelectric bending generator, we can determine the power that can be harvested from the beam. Note that the piezoelectric generator data is measured at point A in Figure 2, and its amplitude reflects the loading that results from the full-wave rectifier circuit in parallel. The total energy that can be generated by the circuit neglecting the losses is given by the following<sup>3</sup>:

$$E_{tot} = \frac{1}{2} CV^2 \quad (6)$$

Thus, by measuring the voltage at position *B* in Figure 2 (load is removed from capacitor bank with the switch) we can estimate the energy stored in the circuit.

Figure 7 is a plot of the calibration of the piezoelectric generator compared to a calibrated strain gauge on the beam. The top plot is an expanded section of the lower plot in Figure 7 and illustrates the phase relationship between the strain data and the piezoelectric voltage as a function of time. In addition, the amplitudes are proportional over the period of the ringing allowing calculation of the direct voltage to

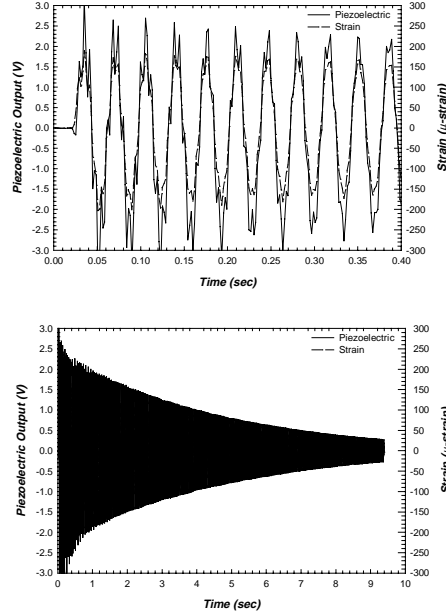
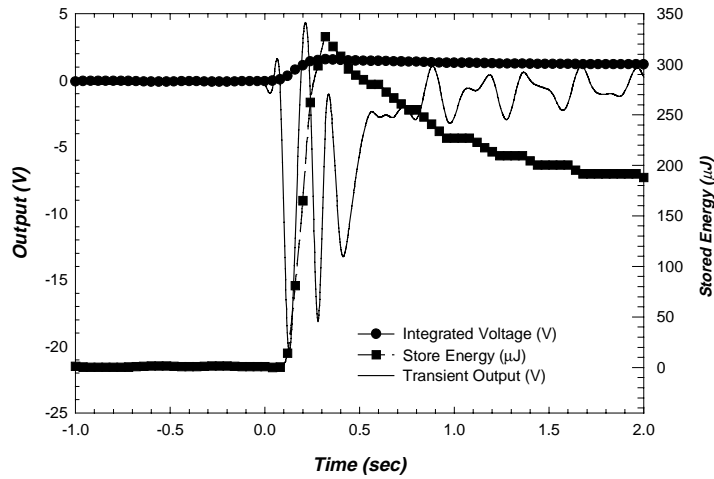


**Figure 7.** Data plot showing relationship between output voltage of piezoelectric and strain on the beam of Figure 6. It is clear that the output is proportional to the strain with a slope of  $\sim 14 \text{ mV}/\mu\text{-strain}$ .

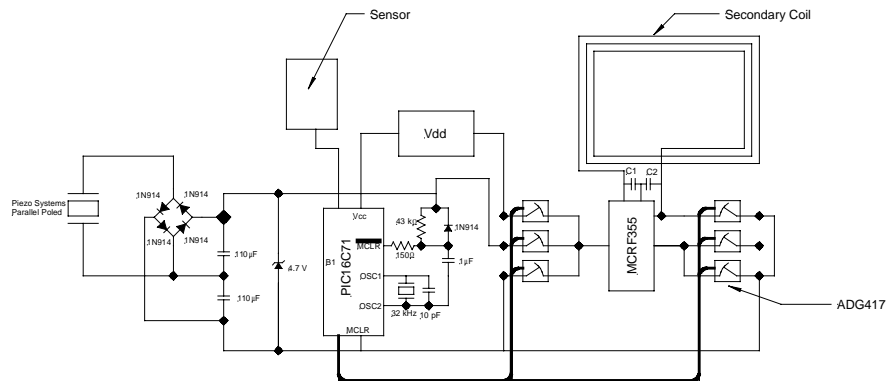
strain conversion factor of  $\sim 14 \text{ mV}/\mu\text{-strain}$ . The bottom plot of Figure 7 illustrates the decay of the signals as a function of time.

Figure 8 is a plot of the transient voltage on the piezoelectric generator (point *A* in Figure 2) and the integrated voltage across the capacitors (point *B* in Figure 2) as a function of time. The total energy stored is also plotted as a function of time and is calculated from Eqn. ( 6). The results of this experiment indicate that approximately  $320 \mu\text{J}$  were stored across the capacitor bank during the single impulse. The droop in the energy plot after 0.4 sec is a result of loading of the circuit by the oscilloscope used to measure the response and leakage of the diodes in the bridge rectifier circuit. Higher quality diodes need to be used to reduce the loss.

The peak integrated voltage observed during the transient was on the order of 1.5 V which we have previously shown to be large enough to drive the microcontroller. The droop rate indicates that peak powers on the order of  $100 \mu\text{W}$  can be delivered and, as noted above, this is enough power to operate the microcontroller for a significant fraction of a second.



**Figure 8.** Plot of response as a function of time for a rapid impulse on a beam. The data plotted as (●) is the voltage across the capacitor bank, the solid line data is the transient voltage output from the piezoelectric generator, and the solid square (■) is the total energy across the capacitor bank. This is the integrated energy for one impulse. To first order, the energy should scale with the number of impulses to the beam. Note that the droop is a result of loading by the oscilloscope with a 1 MΩ input impedance and leakage of the diodes in the bridge rectifier circuit.



**Figure 9.** Block diagram of the self-powered sensor system illustrating contact programming technique and control from the microprocessor.

To first order, each additional mechanical pulse allowing for sustained operation of the repeated impulses. Thus, it is possible for the then store the data with the energy harvested from to the structural element are not periodic but occur truck crossing a bridge, a method must be found to readout before the power stored is consumed.

should add a similar amount of energy to the system microcontroller over many seconds in the case of microcontroller to interrogate a sensor suite and the beam. However, if the repetition of the impulses asynchronously such as in the case of a many axle save the data to non-volatile memory for later

## RF Tag Studies

Recently there has been a large effort in the development of non-contacting radio frequency (RF) tagging technology. These devices function when they are placed in proximity to a reading instrument. The reading instrument is placed a distance from the device and information is transferred from the RF tag to the reader by modulation of the input impedance of the tag. Thus, the back-scattered radiation from the tag is read and interpreted by the powered reading device eliminating the need for batteries or external power to operate the tag.

Work was conducted to determine if RF tagging technology could be implemented to store the data from the sensor to non-volatile memory. Typically, RF tags have flash memory which, along with the identification information, is read out by the system. We chose to test a MicroChip<sup>4</sup> MCRF355 device. This tag operates at 13.56 MHz and has 154 bits available for programming via a contact method. The concept is depicted in Figure 9, which illustrates the technique of using the piezoelectric generator to power the microcontroller, sensor, and write the data to flash EPROM on the RF tag.

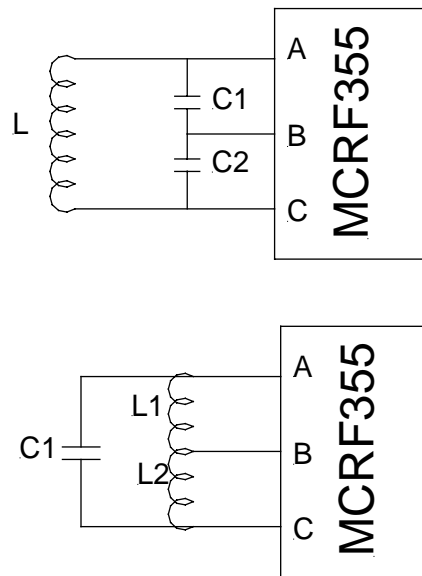


**Figure 10.** Schematic diagram of MCRF355 wired with an RF resonant circuit. Top diagram is for a switched capacitance and the bottom diagram is for a switched inductance system.

In Figure 9, after the voltage is pumped to a level that is sufficient to power the microcontroller, the microcontroller uses its internal analog-to-digital converter (A/D) to make a measurement of the sensor. This data is then placed in the memory of the microcontroller and the data is written to the MCRF355 by opening and closing the ADG417 single-pull single-throw switches. The MCRF355 is wired through to the ADG417<sup>5</sup> devices such that when the power from the piezoelectric device is very low and the system is inactive, the MCRF355 is isolated from the rest of the circuit. This allows the RF tag to operate independently from the rest of the circuit yet be programmed by the rest of the circuit when required. Thus, a measurement can be made by the sensor and stored to the RF tag to be read by a mobile external readout device at a later time even when there is no strain activity in the building member.

One critical aspect of application of RF tags to this application is the ability to produce an RF resonant circuit on a circuit board. This was done by producing a printed circuit board with 3.5 loops of 10 mil traces separated by 10 mil spacings and formed into a 3" square pattern on FR-4 glass for a nominal

inductance of  $4\ \mu\text{H}$ . The inductor was connected to the RF tag in two distinct ways forming a nominally 13.56 MHz resonance. The two approaches are illustrated in Figure 10 where the top schematic is the switched capacitance approach and the bottom schematic is the switched inductance approach. When an electromagnetic signal at 13.56 MHz is near the inductor, the tank circuit tends to adsorb and store energy. This electrical energy is used to power the logic circuits in the MCRF355. The MCRF355 then in turn selectively switches the impedance of pin *B* in Figure 10 such that either  $C2$  or  $L2$  is shorted. This changes the impedance of the tank circuit and the back-scattered energy from the impedance mismatch. Thus, data can be transferred from the MCRF355 to the reader without external power to the MCRF355.

We tested both approaches in Figure 10 with our circuit board and the data is shown in Figure 11. Figure 11 illustrates that the resonance frequency of the tank circuit shifts with the condition of pin *B* of the MCRF355 RF tag. Shifting between the center frequency and the shifted resonance changes the impedance of the tank circuit as viewed from the reader and represents a bit of data. Thus, 154 bits of sensor data can be measured and then read at a much later time, even while there is no strain energy to be harvested and the microcontroller is inactive.

## Conclusion

We have shown that the application of piezoelectric elements to harvest strain from beam elements in critical structures is feasible and could be made practical. We have shown that microcontrollers can be

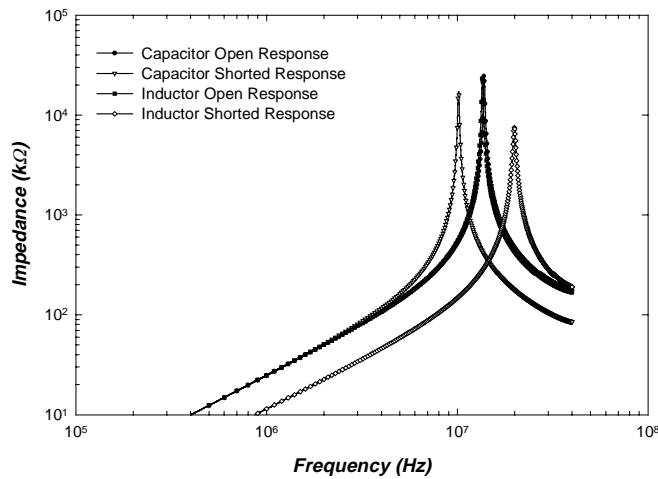


**Figure 11.** Data showing the impedance for circuits in Figure 10 as a function of frequency. The quiescent frequency is 13.56 MHz. Data plotted as a filled circle is the switched capacitor circuit resonance with pin *B* of the MCRF355 inactive. The data plotted as the triangle is the resonance of the switched capacitor circuit when pin *B* is active. The filled square and the open diamond data are for the switched inductor data with pin *B* inactive and active respectively.

operated by power produced from strain only and have demonstrated the conversion and storage of electrical energy produced from this strain. In addition, we have illustrated an approach to storing the data from the sensor to a non-volatile memory and how that data could be retrieved. Thus, the placement of active sensors that do not require external power or wires and are powered by harvesting the stress applied to a building structure is a viable approach to monitoring critical infrastructure.

## REFERENCES

- <sup>1</sup> Piezo Systems, Inc. 186 Massachusetts Ave. Cambridge MA 02139, 617-547-1777.
- <sup>2</sup> C. Germano, *IEE Transaction on Audio and Electroacoustics*, **AU-19**, 1, March 1971.
- <sup>3</sup> J. R. Reitz, F.J Milford, R. W. Christy; *Foundations of Electromagnetic Theory*, 3<sup>rd</sup> Ed., Addison-Wesley, Reading, MA, 1979, pp. 123-124.
- <sup>4</sup> Microchip Technology Inc. 2355 West Chandler Blvd. Chandler, AZ 85224
- <sup>5</sup> Analog Devices, Analog Devices, Inc. Three Technology Way, Norwood, MA 02062.

## Distribution

1	MS 0188	LDRD Office, 4001
1	9018	Central Technical Files, 8945-1
2	0899	Technical Library, 9616
1	0612	Review & Approval Desk, 9612 For DOE/OSTI
5	1425	K. B. Pfeifer, 1744
2	1425	S. K. Leming, 1744
2	1425	A. N. Rumpf , 1744
1	1425	S. A. Casalnuovo , 1744
1	0769	R. V. Matalucci, 5862